Evidence of High Harmonics from Echo-Enabled Harmonic Generation for Seeding X-Ray Free Electron Lasers

D. Xiang, E. Colby, M. Dunning, S. Gilevich, C. Hast, K. Jobe, D. McCormick, J. Nelson, T. O. Raubenheimer, K. Soong, G. Stupakov, Z. Szalata, D. Walz, S. Weathersby, and M. Woodley

Phys. Rev. Lett. **108**, 024802 — Published 11 January 2012

DOI: 10.1103/PhysRevLett.108.024802

Evidence of High Harmonics from Echo-Enabled Harmonic Generation for Seeding X-ray Free Electron Lasers

D. Xiang, E. Colby, M. Dunning, S. Gilevich, C. Hast, K. Jobe, D. McCormick, J. Nelson, T.O. Raubenheimer, K. Soong, G. Stupakov, Z. Szalata, D. Walz, S. Weathersby, M. Woodley
SLAC National Accelerator Laboratory, Menlo Park, CA, 94025, USA

Echo-enabled harmonic generation (EEHG) free electron lasers (FELs) hold great promise in generation of fully coherent radiation in x-ray wavelengths. Here we report the first evidence of high harmonics from the EEHG technique in the realistic scenario where the laser energy modulation is comparable to the beam slice energy spread. In this experiment, coherent radiation at the 7th harmonic of the second seed laser is generated when the energy modulation amplitude is about $2 \sim 3$ times the slice energy spread. The experiment confirms the underlying physics of EEHG and may have a strong impact on emerging seeded x-ray FELs that are capable of generating laser-like x-rays which will advance many areas of science.

PACS numbers: 41.60.Cr

Free electron lasers (FELs) can provide tunable high-power coherent radiation which is enabling forefront science in various areas. At x-ray wavelengths, most of the FELs operate in the self-amplified spontaneous emission (SASE) mode [1, 2]. One FEL working in the SASE mode has been operated at hard x-ray wavelengths [3], which marks the beginning of a new era of x-ray science [4–6]. However, since SASE FEL radiation starts from beam shot noise, the FEL output has limited temporal coherence (i.e. noisy in both temporal profile and spectrum). FELs with improved temporal coherence (i.e. a well-controlled pulse shape and a bandwidth close to transform limit) should benefit many applications and enable new science in spectroscopic studies of correlated electron materials.

Various techniques [7–14] have been proposed to improve the FEL temporal coherence. In the self-seeding scheme, a monochromator is used to purify the spectrum of a SASE FEL and an additional undulator is employed to amplify the purified radiation to the GW level. However, suffering from the intrinsic chaotic properties of the SASE radiation in the first undulator, the monochromated radiation has large intensity fluctuations which may affect the stability of the final output. Furthermore, it is difficult to synchronize the FEL output from the self-seeding scheme to external lasers, which is generally required in pump-probe experiments. Alternatively, seeding with an external source generated from an external laser may provide a fully coherent output having well-defined timing with respect to the laser. One way to directly seed an FEL is to use the high harmonic generation (HHG) source generated when a high power laser is injected to a noble gas. While seeding at 160 nm [8] and 61 nm [9] from a HHG source have been demonstrated, seeding with HHG source in the x-ray wavelength still requires major progress in laser technology.

To circumvent the need for a high power laser at short wavelength, several frequency up-conversion techniques [10–14] have been envisioned to convert the external seed to shorter wavelengths. In the classic high-gain harmonic generation (HGHG) scheme, a single modulator-chicane system is used to bunch the beam at the harmonic frequency of the seed laser [10]. While being simple, the HGHG scheme is characterized by a limited frequency up-conversion efficiency such that generation of the hth harmonic requires the energy modulation ΔE to be roughly h times larger than the beam slice energy spread σ_E. This hinders reaching x-rays from a UV seed laser in a single stage because when a large ΔE is used to generate sufficient bunching at the required high harmonics, the final beam energy spread will be too large to provide sufficient FEL gain at that wavelength.

The frequency multiplication efficiency can be greatly improved with the recently proposed echo-enabled harmonic generation (EEHG) technique [12, 13]. In this scheme, an electron beam is first energy modulated by a laser with wave number k_1 and then sent through a chicane with strong momentum compaction after which the modulation is macroscopically smeared. Simultaneously, separated energy bands with a spread much smaller than the initial energy spread are introduced into the beam phase space. It turns out that if a second laser with wave number k_2 (k_2 can equal k_1) is further used to modulate the beam, density modulation at the wave number

$$k_E = nk_1 + mk_2\,, \tag{1}$$

can be generated (n and m are integers) after passing through a second chicane. The key advantage of EEHG is that by trading the large energy modulation from a laser with a large momentum compaction from a chicane, high harmonics can be generated from those separated energy bands with a relatively small energy modulation. Thus it promises both bunching and gain at very high harmonics, allowing the generation of coherent x-rays directly from a UV seed laser in a single stage.

The potentially high frequency up-conversion efficiency has stimulated world-wide interest in using the EEHG scheme to seed x-ray FELs [15–18]. In recent proof-of-principle experiments performed at SLAC's Next Linear Collider Test Accelerator (NLCTA) [14, 19] and the

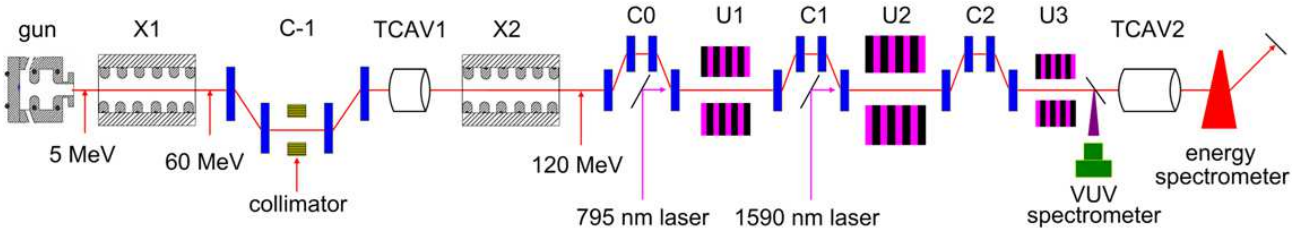

FIG. 1: Schematic of the EEHG experiment at SLAC. Two transverse cavities (TCAV1 and TCAV2) were installed to control the beam slice energy spread and measure the laser energy modulation to benchmark EEHG theory.

SDUV-FEL at SINAP [20], the 4th and 3rd harmonics from EEHG have been observed. These experiments demonstrated that a long-term memory of the beam phase space correlations could be properly controlled and preserved. However, with the energy modulation one order of magnitude larger than the beam slice energy spread, these experiments were incapable of confirming the main advantage of EEHG over HGHG, which is the capability of EEHG to generate high harmonics when the energy modulation is comparable to the slice energy spread. In this Letter, we present the first evidence of high harmonics from the EEHG technique in this regime.

The novelty in our experiment is that a radio-frequency (rf) transverse cavity (TCAV) is used to increase the slice energy spread by one order of magnitude such that the ratio of energy modulation to energy spread is similar to that in real seeded x-ray FELs. In our experiment, the 7th harmonic of the second laser at 227 nm is generated when the energy modulation is approximately $2 \sim 3$ times the slice energy spread.

The layout of the experiment at SLAC's NLCTA is schematically shown in Fig. 1. The electron beam is generated in a photocathode rf gun and is boosted to 60 MeV in an x-band linac (X1). After passing through a chicane (C-1), the beam slice energy spread is increased in a recently installed 11-cell x-band TCAV (TCAV1) and the beam is further accelerated to 120 MeV in the second x-band linac (X2). The beam then enters the EEHG beam line of which the main components are 3 chicanes (C0, C1 and C2) and 3 undulators (U1, U2 and U3). A 27-cell x-band TCAV (TCAV2) downstream of the EEHG beam line allows measurements of the beam longitudinal phase space and laser energy modulations.

In the EEHG beam line, the chicane C0 is used to generate an orbit bump to inject the 795 nm laser into the first undulator U1. After passing through C1, the beam longitudinal phase space is split into many separated energy bands. The beam is again modulated by the 1590 nm laser in the second undulator U2, and after passing through C2, density modulation at shorter wavelengths is generated when the separated energy bands are converted into separated current bands. The bunched beam is finally sent through the third undulator U3 which is tuned to 227 nm to generate coherent radiation at the 7th harmonic of the second seed laser. The radiation generated in U3 is reflected out by an optical transition radiation (OTR) screen and guided to a vacuum UV (VUV) spectrometer (the OTR from the screen itself is measured as well).

The critical element that allows the EEHG technique to be tested in the realistic scenario is a short TCAV which is an rf structure operating in the TM10 mode. For a particle with coordinates $(x_0, x_0', y_0, y_0', z_0, \delta_0)$ passing through a TCAV at the zero-crossing phase, the divergence changes to $x_1' = x_0' + kz_0$, where $k = 2\pi eV/\lambda_{rf}E$ is the dimensionless kick strength, V is the voltage of the cavity, E is electron energy and λ_{rf} is the wavelength of the rf field. This time-dependent angular kick makes a TCAV well suited for the measurement of bunch temporal profiles [21, 22]. Another less prominent effect associated with a TCAV is that a particle's relative energy deviation will change to $\delta_1 = \delta_0 + kx_0$, as dictated by the Panofsky-Wenzel theorem [23]. The energy change is from the longitudinal electric field which varies linearly with transverse distance. As a result, the TCAV will increase the beam slice energy spread by $\sigma_{E,T} = k\sigma_x E$, where σ_x is the rms beam size in the cavity, similar to a conventional laser heater [24].

In our experiment, the 7th harmonic at 227 nm corresponds to the set $n = -2$ and $m = 11$ as illustrated in Eq. (1). Operating EEHG in the $n = -2$ regime has the advantage that the required momentum compaction for the first chicane is roughly a factor of 2 smaller than that required in the nominal $n = -1$ and $m = 9$ case, though the bunching is slightly lower [16, 17]. The laser energy modulations are controlled with wave plates and set at about 20 keV and 15 keV in the 1st and 2nd modulators, respectively. The momentum compaction of the chicanes were accordingly set at $R_{56}^{(1)} = 7.53$ mm and $R_{56}^{(2)} = 3.71$ mm to maximize the bunching at the 7th harmonic.

The laser energy modulation is estimated through the measurement of the coherent optical transition radiation (COTR) intensity at 795 nm after C2. For HGHG, the bunching factor at various harmonic number is [10],

$$b_h = |J_h(2\pi h R_{56}\Delta E/\lambda E)| e^{-\frac{1}{2}(2\pi h R_{56}\sigma_E/\lambda E)^2}. \quad (2)$$

where h is the harmonic number and λ is the wavelength of the modulation. Eq. (2) implies that for a given R_{56} the bunching factor oscillates as a function of energy modulation, as dictated by the Bessel function in Eq. (2). Therefore, the energy modulation can be obtained through the measurement of the COTR intensity which is proportional to b_h^2 by scanning the laser energy.

As an example, with C2 set at $R_{56}^{(2)} = 3.71$ mm and the 1590 nm laser turned on, the measured COTR intensity with a bandpass filter centered at 795 nm for various wave plate angles (laser energy scales as $\sin^2(2\theta)$) is shown in Fig. 2a. Note in our experiment the laser pulse width is shorter than the electron beam, so the energy modulation amplitude and the corresponding bunching varies along the beam. Since the measured signal is the integrated radiation over the whole bunch, the contrast of the oscillation for various laser energy is reduced. Nevertheless, by comparing the measurement with theory that takes into account the variation of the energy modulation allows us to roughly set the laser energy to provide the desired energy modulation. For instance, a comparison between the data and theory indicates that the wave plate should be set at about 30 degrees to provide a peak energy modulation at 15 keV.

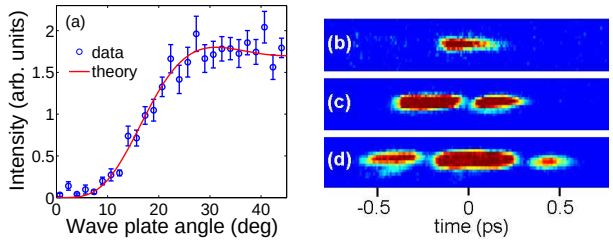

FIG. 2: (a) COTR intensity vs wave plate angle; (b), (c), (d) are the time-resolved COTR intensities with $R_{56}^{(2)}$ set to 3.2 mm, 5.2 mm and 6.2 mm, respectively.

A more precise determination of the energy modulation was obtained through a time-resolved measurement of the COTR intensity using TCAV2 and a downstream OTR screen [25]. In our experiment, the density-modulated beam is streaked vertically with TCAV2 and the time-dependent COTR intensity was measured at various $R_{56}^{(2)}$ (Fig. 2b, c, d). The results indicate that by measuring the time-dependent COTR signal with a TCAV, the oscillation of the bunching as a function of energy modulation can be well resolved. A comparison between the measured COTR oscillation and Eq. (2) yields good agreement and the peak laser modulation is found to be 15.5 ± 1.0 keV.

After the laser energies are set to provide the desired energy modulation, we first turned on the 1590 nm seed laser and the 7th harmonic at 227 nm from HGHG was observed (the beam slice energy spread is estimated to be well below 1 keV from simulation). As we gradually increase TCAV1 voltage, the HGHG signal decreased as a result of the enhanced suppression effect from the slice energy spread, as illustrated in Eq. (2). The measured radiation at 227 nm for various TCAV1 voltage is shown in Fig. 3. From Fig. 3 one can see that increasing the voltage of TCAV1 to 255 kV completely suppressed the 7th harmonic from HGHG. By fitting the coherent radiation data to the square of Eq. (2), the beam slice energy spread when TCAV1 voltage is 255 kV is found to be approximately 4.1 keV. It should be pointed out that Eq. (2) is obtained with 1-D theory and the beam energy spread is assumed to be a Gaussian distribution. In our experiment the beam energy spread distribution after TCAV1 largely depends on the beam transverse distribution in TCAV1 and is likely to have a complicated distribution. This is because the experiment is performed in a low charge mode and the non-uniformity of both the cathode drive laser and the cathode quantum efficiency leads to many 'hot spots' in the beam transverse distribution which is not smeared out by space charge forces. Accordingly, the value estimated using Eq. (2) should be considered as the lower limit of the beam slice energy spread.

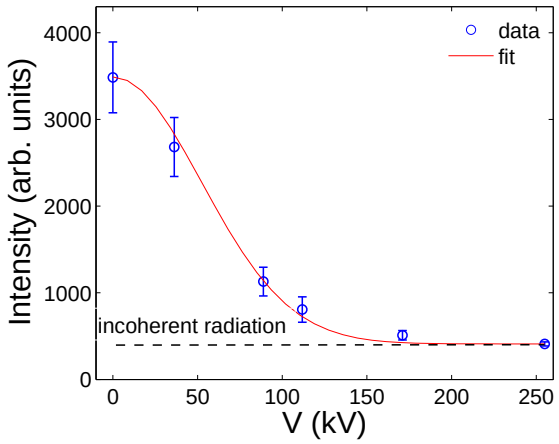

FIG. 3: 227 nm coherent radiation intensity vs TCAV1 voltage when only the 1590 nm laser is on.

For another independent estimate of beam slice energy spread, a screen was inserted just upstream of TCAV1 to obtain the beam size. Note, it is the slice beam size rather than the projected beam size that determines the slice energy spread growth. To estimate the slice beam size, the beam was accelerated slightly off-crest in X1 (beam energy correlates with time) and a collimator with 1 mm aperture in the center of C-1 (see Fig. 1) was used to select a short beam slice of which the size is measured to be about 0.15 mm. Considering this value as the upper limit of the true slice beam size, the corresponding upper value of the slice energy spread was estimated to be about 9.1 keV when TCAV1 voltage is 255 kV.

Given the lower limit 4.1 keV and the upper limit 9.1 keV mentioned above (for $V = 255$ kV), in what follows, the beam slice energy spread at 255 kV will be quoted as $\sigma_{E,T} = 6.6$ keV as the median of the estimated lower and upper values. For beam slice energy spreads at other TCAV1 voltages, we linearly scale $\sigma_{E,T}$ with V.

Representative spectra for various beam slice energy spreads obtained with various TCAV1 voltages are shown in Fig. 4. The spectra were measured with a VUV spectrometer which consists of a 300 line/mm grating and a UV sensitive CCD detector. The spectrometer was cal-

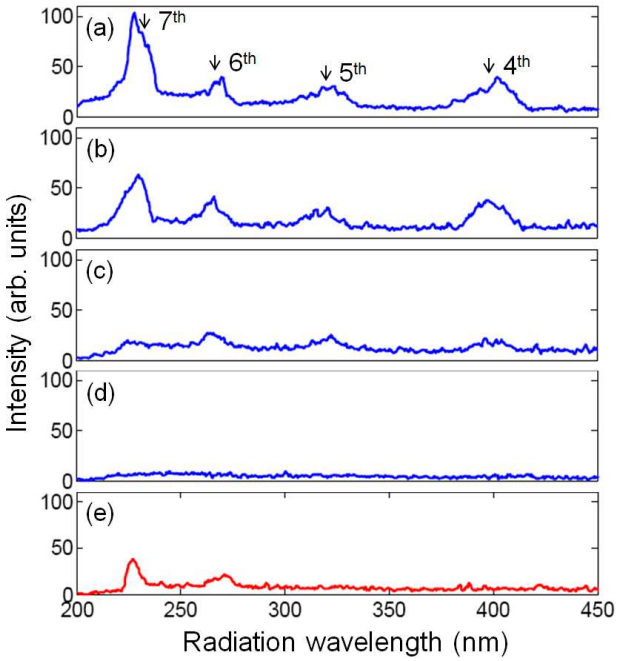

FIG. 4: Spectrum of the radiation for various beam slice energy spreads: (a) below 1 keV; (b) 2.2 keV; (c) 4.4 keV; (d) and (e) 6.6 keV. The beam slice energy spreads are varied by changing TCAV1 voltages. (a)-(d) are the HGHG signals when only the 1590 nm laser is on and (e) is EEHG signal with both lasers on.

ibrated with a Hg(Ar) lamp. A slit with 0.5 mm width is used at the entrance to the spectrometer to reduce the radiation source size. The corresponding resolution of the spectrometer was about 4 nm.

Fig. 4(a) through Fig. 4(d) were HGHG spectra obtained with only the 1590 nm laser on and Fig. 4(e) is obtained with both lasers on. The spectrum of the coherent radiation is broadened in our experiment due to the relatively large residual energy curvature from the varying rf phase along the bunch. As can be seen from Fig. 4, the harmonic radiation intensity decreases as the beam slice energy spread is increased. Generally speaking, higher harmonics are more sensitive to the energy spread increase, as illustrated in Eq. (2). When the beam slice energy spread is increased to 6.6 keV, the 4th to 7th harmonics are all suppressed and only the incoherent radiation was observed (Fig. 4(d)). When the first seed laser at 795 nm is turned on, the 6th and 7th harmonics from the EEHG process are generated, as can be clearly seen in Fig. 4(e).

According to Eq. (2), increasing the beam slice energy spread from 1 keV to 6.6 keV will reduce the HGHG bunching factor at the 7th harmonic from about 20% to the shot noise level (10^{-3}). With the first laser at 795 nm turned on, the EEHG theory predicts that the 7th harmonic bunching of about 10% can be generated. Analysis that takes into account the realistic experimental condition implies that the integrated EEHG signal at the 7th harmonic in Fig. 4(e) should be about a factor of 2 smaller than the HGHG signal in Fig. 4(a). In the experiment, the observed EEHG signal is, however, about a factor of 3 smaller than the HGHG signal. This is likely due to the limited acceptance of the VUV spectrometer and the increased transverse beam size in U3 because the beam was spatially chirped with TCAV1 on.

The suppression of high harmonics in the frequency domain can be understood as smearing of fine structures in the time domain. Consider a beam with vanishing bunch length but a spread in energy σ_E, after going through a chicane with momentum compaction R_{56}, the spread in energy is converted to a spread in time. As a result, the beam ends up with an rms duration $R_{56}\sigma_E/E$. With the first laser off, the increased energy spread from TCAV1 together with the momentum compaction of C2 effectively washes out any structures that are finer than $\pi R_{56}^{(2)}\sigma_{E,T}/E \approx 600$ nm. With the first laser on, the energy modulation ΔE_1 together with the large momentum compaction of C1 split the beam phase space into separated energy bands with spreads a factor of $k_1 R_{56}^{(1)}\Delta E_1/E$ (about 10 in this experiment) smaller than $\sigma_{E,T}$, allowing the 7th harmonic to be produced via the EEHG process.

Note, in the regime when energy modulation is comparable to slice energy spread, the harmonic number that can be achieved in EEHG technique is comparable to $k_1 R_{56}^{(1)}\Delta E_1/E$. To scale to soft x-ray wavelength (say, 5 nm), one needs to increase this factor to about 50 starting with UV seed lasers. Assuming a 1.2 GeV beam (120 MeV in our experiment) and 266 nm UV seed laser (795 nm in our experiment) similar to the parameters in the FERMI FEL [16] under construction in Italy, given the same momentum compaction (7.53 mm) as in our experiment, one may accordingly increase ΔE_1 to 330 keV (20 keV in our experiment) to increase this factor to 50 to reach the soft x-ray wavelength at the 50th harmonic. In contrast, with such a small energy modulation, the harmonic number achievable in HGHG is limited to $2 \sim 3$ (assuming 150 keV slice energy spread).

In summary, we have presented the first evidence of high harmonics from the EEHG technique which overcomes the limit arising from the beam slice energy spread. Our result is a clear signature that by splitting the phase space with a large momentum compaction chicane, high harmonics can be generated with relatively small energy modulation. This experiment also demonstrated that the current technology was able to provide the required accuracy in controlling the beam dynamics in EEHG and indicate that EEHG presents a feasible option for future seeded x-ray FELs.

We thank C. Adolphsen, S. Chu, F. Wang and J. Wang for construction and test of the transverse cavities and J. Rzepiela for help in data acquisition. This work was supported by the US DOE Office of Basic Energy Sciences using the NLCTA facility which is partly supported by US DOE Office of High Energy Physics under Contract No. DE-AC02-76SF00515.

[1] A. Kondratenko and E. Saldin, Part. Accel. 10, 207 (1980).
[2] R. Bonifacio, C. Pellegrini, and L.M. Narducci, Opt. Commun. 50, 373, (1984).
[3] P. Emma, *et al.*, Nat. Photon. 4, 641 (2010).
[4] L. Young *et al.*, Nature 466, 56 (2010).
[5] H. Chapman *et al.*, Nature 470, 73 (2011).
[6] M. Marvin Seibert *et al.*, Nature 470, 78 (2011).
[7] J. Feldhaus *et al.*, Opt. Commun. 140, 341 (1997).
[8] G. Lambert *et al.*, Nat. Phys. 4, 296 (2008).
[9] T. Togashi *et al.*, Opt. Express 19, 317 (2011).
[10] L.-H. Yu, Phys. Rev. A 44, 5178 (1991).
[11] L.-H. Yu, *et al.*, Science 289, 932 (2000).
[12] G. Stupakov, Phys. Rev. Lett. 102, 074801 (2009).
[13] D. Xiang and G. Stupakov, Phys. Rev. ST Accel. Beams 12, 030702 (2009).
[14] D. Xiang *et al.*, Phys. Rev. Lett. 105, 114801 (2010).
[15] D. Xiang and G. Stupakov, in *Proceedings of PAC 09, Vancouver* (IEEE, New York, 2009).
[16] E. Allaria, *et al.*, in *Proceedings of FEL 09, Liverpool* (2009), p.39.
[17] S. Reiche *et al.*, in *Proceedings of FEL 09, Liverpool* (2009), p.51.
[18] H. Deng, W. Decking and B. Faatz, arXiv:1103.0112, (2011).
[19] P. Zeitoun, M. Fajardo and G. Lambert, Nat. Photon. 4, 739 (2010).
[20] Z. Zhao *et al.*, in preparation, (2011).
[21] G. Berden *et al.*, Phys. Rev. Lett. 99, 164801 (2007).
[22] K. Bane *et al.*, Phys. Rev. ST Accel. Beams 12, 030704 (2009).
[23] W. Panofsky and W. Wenzel, Rev. Sci. Instrum. 27, 967 (1956).
[24] Z. Huang *et al.*, Phys. Rev. ST Accel. Beams 13, 020703 (2010).
[25] D. Xiang *et al.*, submitted to Phys. Rev. ST Accel. Beams (2011).